Applied Geochemistry 97 (2018) 197–208

Contents lists available at ScienceDirect

Applied Geochemistry

journal homepage: www.elsevier.com/locate/apgeochem

Time series analysis of soil radon in Northern Pakistan: Implications for earthquake forecasting

Adnan Barkat[a,*], Aamir Ali[b], Umar Hayat[c], Quentin G. Crowley[d], Khaista Rehman[e], Naila Siddique[f], Takreem Haidar[c], Talat Iqbal[a]

[a] Centre for Earthquake Studies, National Centre for Physics, Islamabad, Pakistan
[b] Department of Earth Sciences, Quaid-i-Azam University, Islamabad, Pakistan
[c] Department of Mathematics, Quaid-i-Azam University, Islamabad, Pakistan
[d] Department of Geology, School of Natural Sciences, Trinity College, Dublin 2, Ireland
[e] National Centre of Excellence in Geology, University of Peshawar, Pakistan
[f] Chemistry Division, Directorate of Science, PINSTECH, Islamabad, Pakistan

ARTICLE INFO

Editorial handling by Prof. M. Kersten

Keywords:
Earthquake precursors
Radon
Radionuclides
Hurst exponent
Northern Pakistan

ABSTRACT

Time series analysis of soil radon data has previously been proposed as a mechanism for earthquake hazard forecasting, but it is not universally accepted as such. Here we perform time series analysis of soil radon along an active fault zone in North Pakistan, in order to investigate pre-earthquake anomalies for a period of July 24, 2014 to April 30, 2015. The methodology includes geochemical analysis of soil, deterministic analysis (Hurst exponent *H*), quantification of meteorological influence and abnormalities of soil radon within the context of earthquake forecasting. In particular, for analyzing abnormalities in radon data, we have used residual signal processing techniques to reduce the regular effect of meteorological factors and a statistical criterion ($\bar{x} \pm 2\sigma$) at a 95% confidence interval. Results of geochemical analysis suggest that any abnormal enhancement in soil radon concentration is not associated with the presence of key radionuclides such as ^{226}Ra, ^{232}Th and ^{40}K. The deterministic analysis of radon and meteorological parameters reveals that H belongs to the interval $0.5 \leq H \leq 1$, which indicates a persistent trend with insignificant infrequency and irregularity. Likewise, the influence of meteorological parameters on soil radon is quantified via correlation coefficients suggesting an insignificant impact. Furthermore, temporal variability of residual radon around the time of earthquake activity reveals the presence of six notable anomalous peaks overpassing the statistical criterion during the investigated period. An absence of anomalous residual radon behavior for some earthquake events in the investigated period can be attributed to their low magnitude and high R_E/R_D value. Finally, our results validate earlier findings and recommend the use of radon as a seismic indicator.

1. Introduction

Contemporary earthquake seismology indicates that migration of soil gases mainly depends on the availability of favorable subsurface structures (Walia et al., 2013; Tarakçı et al., 2014; Woith, 2015; Wang et al., 2017; Barkat et al., 2018; Yan et al., 2018). These structures include faults and fractures facilitating the migration of soil gases upward from deeper horizons (Choubey et al., 2007; Yuce et al., 2017). Systematic monitoring of soil gases in seismically active regions is of possible benefit within the context of earthquake forecasting (Pulinets and Ouzounov, 2011). The existence of a potential correlation between variability of soil gases and impending earthquakes has been reported in several studies (Pulinets and Boyarchuk, 2004; Vaupotic et al., 2010; Huang et al., 2017; Awais et al., 2017; Barkat et al., 2018).

Among all the terrestrial gases such as *Rn, H_2, He, CO_2, CH_4, Ar, O_2* and N_2, ^{222}Rn has been most extensively studied within the context of earthquake forecasting due to its unique geochemical characteristics (Sugisaki, 1978; Hartmann and Levy, 2005; Fu et al., 2017a). These characteristics include its easy detectability, short half-life (3.82 days) and inert nature. The variability of soil radon is influenced by lithology, soil porosity, radionuclide composition and meteorological parameters such as temperature, pressure, humidity and rainfall (Fujiyoshi et al., 2006; Barbosa et al., 2007; Kikaj and Vaupotič, 2017). Moreover, in some cases a radon isotope (thoron: ^{220}Rn) is also used within the above context despite having shorter half-life (55.6 s) (Yang et al., 2005; Oh and Kim, 2015).

* Corresponding author.
E-mail address: adnan.barkat@ncp.edu.pk (A. Barkat).

https://doi.org/10.1016/j.apgeochem.2018.08.016
Received 10 January 2018; Received in revised form 16 August 2018; Accepted 20 August 2018
Available online 28 August 2018
0883-2927/

The investigation of radon in different environments i.e. soil, air and water in the context of earthquake forecasting is reported in numerous studies (Fujiyoshi et al., 2006; Planinic et al., 2004; Ghosh et al., 2009; Tarakçı et al., 2014; Oh and Kim, 2015; Singh et al., 2017). Radon anomalies can appear a few days or weeks prior to the impending seismic events (Planinić et al., 2001; Riggio and Santulin, 2015). For example, a radon anomaly was registered prior to the Tashkent (Uzbekistan) earthquake (M 5.5; 1966) with a several-fold in soil radon concentration (Arora et al., 2017). An anomalous increase of radon concentration in ground water was also reported prior to Izu-Oshima-Kinkai (1978) and Kobe (1995) earthquakes (Fu et al., 2017a).

The correlation of radon anomalies with seismic activity requires careful analysis of crucial factors affecting its concentration (Walia et al., 2013; Tarakçı et al., 2014; Oh and Kim, 2015; Awais et al., 2017; Jilani et al., 2017). These factors can be summarized as meteorological parameters (i.e. temperature (T), pressure (P), rainfall and relative humidity (rH)). Furthermore, identification of possible correlation between variability of soil radon and the concentration of naturally occurring radionuclides requires geochemical analysis of soil (Bem et al., 1998; Forkapic et al., 2017). It is also very important to examine the dynamics of radon time series, determine the degree of chaotic behavior, and prediction of future variations and investigate their correlation with meteorological parameters (Planinic et al., 2004; Barbosa et al., 2007; Nikolopoulos et al., 2014; Li et al., 2016).

This study aims to undertake a statistical analysis of the temporal variability of soil radon near a seismically active location (33.742°N, 73.065°E) in Islamabad (North Pakistan) using fractal methods for a selected time window of July 25, 2014 to April 31, 2015. A further aim is to correlate the pre- co- and post-seismic signal registered by local and global seismic networks using radon anomalies (Table 1). A number of methodologies have been applied to test the hypothesis that temporal variation of soil radon can be used as a viable indicator of seismic activity.

1. Detailed geochemical (e.g. measurement of ^{226}Ra, ^{232}Th, ^{40}K and other radionuclides) and physicochemical (e.g. moisture content, pH and conductivity) analyses of local soil are presented.
2. The fluctuation of radon concentration with the atmospheric/soil meteorological parameters obtained from the Pakistan Meteorological Department (PMD) and the radon monitor (RTM 2200) for the selected time window are presented and analyzed.
3. Fractal analysis of radon is performed to distinguish between chaotic behavior (deterministic chaos) and noise (radon fluctuations) and its controlling meteorological parameters for the selected time window.
4. Statistical averaging is applied to the radon time series to eliminate the regular effect of meteorological parameters for the improved and reliable identification of radon anomalies possibly associated with the impending seismic activity. Then a statistical criterion ($\bar{x} \pm 2\sigma$) for identification of anomalous behavior is applied on residual radon concentration obtained using the difference between radon concentration and its rolling average. The statistical bound applied in this study for anomaly selection is consistent with other studies (Vaupotic et al., 2010; Oh and Kim, 2015).
5. The declared anomalous zones of radon are correlated with seismic activity in the selected time window and the results are compared with earlier findings reported by Jilani et al. (2017) and Barkat et al. (2017).

In what follows, we present seismo-tectonic setting of the study area, highlighting its importance within the context of earthquake forecasting.

2. Tectonics of the study area

The seismo-tectonic of Pakistan is characterized by the continental collision between the Indian and Eurasia plates (Molnar and Tapponnier, 1975; Ali et al., 2009; Tahir and Grasso, 2013; Rehman et al., 2015,2017b; Asim et al., 2017). Movement of these two plates is responsible for the occurrence of major earthquakes in and around Northern Pakistan. According to Kearey et al. (2013) and Faisal et al. (2014), the Himalayas in North Pakistan which extend from Afghanistan in the west to Myanmar in the East, formed due to continental collision of the above two plates. The major structural trends of Northern Pakistan include, from north to south, the Main Karakoram Thrust (MKT), the Kohistan Island Arc (KIA), the Main Mantle Thrust

Table 1
List of earthquake events used in present study for precursory analysis.

Time	Latitude	Longitude	Depth	Magnitude	R_D	R_E	R_E/R_D
(MM:DD:YYYY)	(°N)	(°E)	(km)	(M)	(km)	(km)	
08/02/2014	33.904	72.419	35.00	4.1	57.94	62	1.08
08/19/2014	34.579	71.002	44.40	3.3	26.242	211	8.04
08/22/2014	34.973	72.994	18.00	3.7	19.50	137	7.02
08/31/2014	36.586	71.090	189.85	5.4	209.89	364	1.73
09/11/2014	32.397	71.237	10.00	4.0	52.48	227	4.32
09/13/2014	36.618	69.680	130.55	5.5	231.74	444	1.91
09/22/2014	34.294	73.919	26.73	4.7	104.95	100	0.95
09/23/2014	34.815	73.393	42.10	3.5	31.99	123	3.85
10/14/2014	36.580	70.930	160.00	5.5	231.74	370	1.60
10/23/2014	34.915	73.878	34.56	4.8	115.88	150	1.30
11/09/2014	36.972	70.776	175.70	5.3	190.11	415	2.18
12/21/2014	34.910	73.843	41.11	4.2	63.97	148	2.32
01/31/2015	32.604	73.939	27.00	3.3	26.24	151	5.74
02/05/2015	34.018	74.011	31.00	3.5	31.99	96	3.01
02/24/2015	34.321	73.663	59.79	3.7	38.99	85	2.17
02/26/2015	34.671	73.278	29.74	5.4	209.89	105	0.50
02/27/2015	34.594	73.380	32.59	4.2	63.97	99	1.55
02/27/2015	34.548	73.307	27.37	4.0	52.48	92	1.76
02/27/2015	34.596	73.334	26.86	4.2	63.97	98	1.53

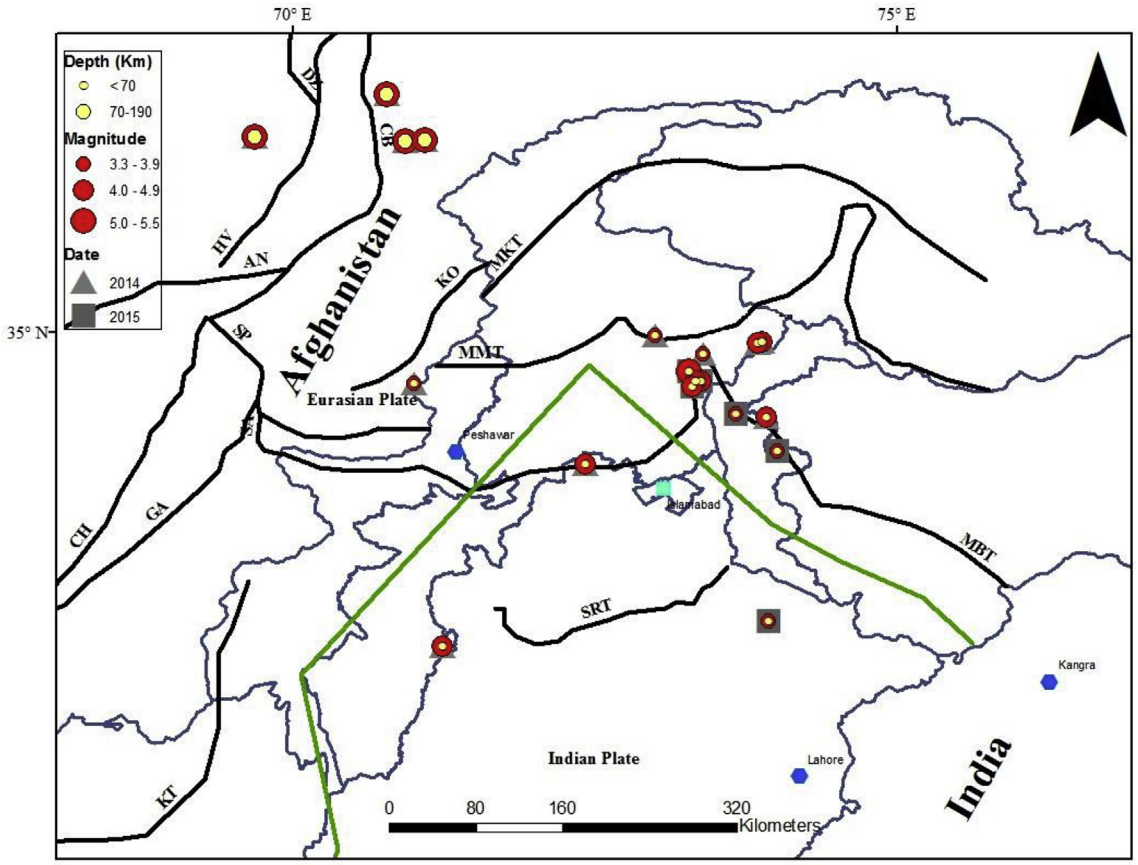

Fig. 1. A simplified sketch of regional tectonics and distribution of earthquakes along with the location of soil radon monitoring station (Blue square). Blacklines denote major faults. Abbreviations of fault names: AN, Andarab, CB, Central Badakhsan, DZ Darvaz, GA Gardez, HV Henjvan, KO Konar, KT Kurram Thrust, MBT Main Boundary Thrust, MKT Main Karakoram Fault, MMT Main Mantle Thrust, SA Sarobi, SP Spinghar. Thick blue lines indicate location of the Indian and Eurasian plates (modified after Kazmi and Jan 1997 and Rehman et al., 2015). Blue hexagon indicates the cities in and around Pakistan. (For interpretation of the references to colour in this figure legend, the reader is referred to the Web version of this article.)

(MMT), the Nanga Parbat-Haramosh Syntaxis, Hazara Kashmir Syntaxis, Main Boundary Thrust (MBT) and the Salt Range Thrust (SRT) (Fig. 1; Kazmi and Jan 1997; Ali et al., 2009; Rehman et al., 2015). Fig. 1 shows that many earthquake epicenters are located in and around the Hazara-Kashmir Syntaxis during the selected time window. Fig. 1 also shows that these earthquakes are shallow seismic events (Depth = 0–70 km) that originated along the MBT. Numerous intermediate-depth earthquakes (Depth > 70 km) delineate the high seismic zone of Hindu Kush, lying in the Afghan-Pakistan border (Rehman et al., 2017a).

Pakistan is ranked 5th in population size category in 2017 with over 200 million inhabitant. Many major populated cities of Pakistan are located on or near active fault zones. The capital of Pakistan, Islamabad is located in the proximity of active fault of the MBT and other faults (Riwat Fault, Jhelum Fault, Kalabagh Fault, Mansehara Fault and the Kotli Thrust). The MBT is a key tectonic element which is responsible for destructive earthquakes e.g., Kashmir Earthquake (*M 7.6*) Oct 8, 2005 (34.29°N, 73.37°E).

3. Methodology

3.1. Experimental setup

3.1.1. Radon monitor

In the present study, soil radon and thoron along with soil meteorological parameters were continuously measured using the RTM 2200, which was installed by the Centre for Earthquake Studies (CES National Centre for Physics, Islamabad, Pakistan) at Islamabad; Saidpur village monitoring site (Fig. 1). For establishing a radon monitoring site, a soil probe was fixed at 1 m depth in the soil profile and encased with a PVC pipe to avoid any infiltration of rainfall. The top soil was covered with a polythene sheet in order to minimize atmospheric effect. The subsoil radon is transported via a section pump to the chamber through a surgical pipe. The sensitive volume and the sensitivity of the detector are 0.27 L and 0.01 cpm per Bq/m^3 respectively, determined by comparing it with the reference instrument having a statistical error of ± 1%. Real time measurements of radon/thoron and soil meteorological parameters (temperature, pressure and relative humidity) were measured every 15 min. The instrumental setup used in the current study is also utilized globally within the context of earthquake forecasting. Further details on this instrumental setup, can be found in Fu et al. (2017a) and Jilani et al. (2017).

3.1.2. Geochemical analysis of soil

A detailed geochemical analysis of soil around the monitoring site was performed to know the content of naturally occurring radionuclides using Gamma Spectroscopy along with other soil properties i.e. moisture content, pH and conductivity. The purpose of this detailed geochemical analysis is to access the content of the natural and anthropogenic radionuclides ^{238}U, ^{232}Th, ^{40}K and ^{137}Cs that affect the radon level. In particular, soil samples were collected, mixed and homogenized from the proximity of the radon monitor at a depth of ~1 m, dried and used in powdered form with the help of sieving. After that, the soil was sealed and stored for 4–6 weeks in order to attain secular equilibrium (Siddique et al., 2006).

The Gamma spectroscopic measurement for radionuclide analysis

was performed using High Purity Germanium (HPGe; Canberra Model AL-30) detectors on a dry weight basis. The detection system has a resolution of 1.9 keV for the 1332.5 keV peak of ^{60}Co and a Peak-to-Compton ratio of 60:1. The software GammaVision, Version 6.01 (Advanced Measurement Technology, Inc.) was used for spectral acquisition. The counting system was calibrated daily using calibrated γ-ray sources. The most abundant γ-peak was used for quantification, whereas the less abundant peaks were used to confirm the presence of a particular radionuclide. All necessary corrections were applied and the final results obtained on a dry weight basis compared with standard references. The brief description of the experimental setup and procedure used for radionuclide analysis is described by Siddique et al. (2006).

3.2. Theoretical setup

3.2.1. Time series analysis of radon

The emanation of soil radon can be considered as a complex and nonlinear stochastic process having dependency on potential chaotic variables i.e. soil temperature, pressure and humidity (Planinic et al., 2004; Barbosa et al., 2007; Külahcı; Şen, 2014). To detect long-range discrepancies and to estimate the temporal evenness of radon time series before correlation with seismic activity, long memory characteristics are needed to be examined. The similarity of fractal dimensions determines the degree of correlation between radon and their controlling parameters (T, P and rH). Long memory characteristics are used to express the dependency of elements on one or more factors over a specific lag (Barbosa et al., 2007; Pausch et al., 1999; Gkarlaouni et al., 2017).

To obtain long-memory effects, R/S analysis of the radon time series is performed in order to define the temporal tendency known as the Hurst exponent (H) whose value ranges from 0 to 1. In particular, H quantifies the stochastic memory of a process related to the fractal dimension. H is classified into three different scenarios into which it may be classified as random, persistent and anti-persistent (Tatli, 2015; Gkarlaouni et al., 2017).

In the first scenario, known as a random walk, H is often close to 0.5 suggesting that the process or time series does not possess long memory trend. In the second scenario, H is in a range of $0.5 \leq H \leq 1$ known as persistent trend. The persistent trend means that the time series exhibits a long memory correlation between events. The third scenario implies an anti-persistent trend if $0 \leq H \leq 0.5$ and a trend reversion is more probable than the trend continuation. According to the R/S method, the set of observations $N \in \{N_1, N_2, N_3, ..., N_n\}$ is further divided into d non-overlapping intervals of N, $(N_{(K-1)S+1}, N_{(K-2)S+2}, ..., N_{K.S})$, whereas $k = 1, 2, 3, \ldots, d$ with individual length $s = n/d$. The computation methodology of H is based on the following relation given by

$$\left(R/S\right)_s = \frac{1}{d}\sum_{k=1}^{d}\left(R_{k,s}/S_{k,s}\right) \tag{1}$$

In Equation (1), $R_{k,s}$ is calculated using the following relationship

$$R_{k,s} = max_{1\leq i\leq s}\{(Y_{k,s})_i\} - min_{1\leq i\leq s}\{(Y_{k,s})_i\} \tag{2}$$

Here $(Y_{k,s})_i$ is the deviation of an individual observation of subgroups (i) from their mean ($\overline{X}_{k,s}$) and calculated as

$$(Y_{k,s})_i = \sum_{j=1}^{i}\left(X_{(k-1)s+j} - \overline{X}_{k,s}\right) \tag{3}$$

The mean ($\overline{X}_{k,s}$) of subgroups can be calculated as

$$\overline{X} = \frac{1}{S}\sum_{i=1}^{s} X_{(k-1)s+i} \tag{4}$$

The parameter $S_{k,s}$ introduced in Equation (1) is calculated using the following relationship

$$S_{k,s} = \sqrt{\sum_{i=1}^{s}(X_{(k-1)s+i} - \overline{X}_{k,s})^2 / s} \tag{5}$$

In conclusion, the rescaled range is linearly regressed against groups according to following relationship

$$log_{10}\left(R/S\right) = constant + H_{obs}\, log_{10} s \tag{6}$$

where H_{obs} is the estimate of the Hurst exponent. In general, for Hurst statistics large data sets (2500 or more observations) are required (Planinic et al., 2004).

3.2.2. Correlation with earthquake activity

Correlation between the anomalous emanation of soil radon and an impending earthquake event is mainly dependent upon the zone of earthquake preparation. The earthquake preparation zone is defined as an area under the influence of tectonic stresses within which the precursory manifestations related to earthquake activity can be observed. Dobrovolsky et al. (1979) proposed a mathematical relationship between the magnitude and the radius of the (respective) event given by:

$$R_D = 10^{0.43M} \tag{7}$$

Here, M is the earthquake magnitude, and R_D is the radius (km) of the preparation zone within which precursory phenomenon may manifest (Dobrovolsky et al., 1979; Vaupotic et al., 2010). The magnitude of the earthquake event plays a crucial role in determining the radius of the preparation zone; whereby earthquakes of greater magnitudes have larger preparation zones and vice-versa. The distance between the earthquake epicenter and the monitoring station is referred to as epicentral distance (R_E). The cut-off value for R_E in this study is taken to be less than or equal to $1.5R_D$ with $M > 3$. This cut-off means that only earthquake events with $M > 3$ and $R_E/R_D \geq 1.5$ possess the potential chance of registering precursors related to them. The criterion for the earthquake preparation zone applied in this study is consistent with other studies performed by Zmazek et al. (2005), Vaupotic et al. (2010), Papastefanou (2010), Laskar et al. (2011), Walia et al. (2013) and Oh and Kim (2015).

In this investigation, we adopted the residual signal processing technique for identification of radon anomalies associated with earthquake activity by reducing the regular frequent effects of recorded data (Fu et al., 2017a; b). This technique uses the comparison of hourly and daily averaged (also known as the trend line for radon concentration) raw radon data with a 7 days rolling average. The residual radon concentration ($dA(t)$) is the difference between daily averaged ($A(t)$) and the 7 days rolling averaged ($RA(t)$) radon concentration presented as:

$$dA(t) = A(t) - RA(t) \tag{8}$$

Anomalous behavior related to the residual radon concentration is determined with the help of a statistically bound (threshold) equal to the mean value ± two times the standard deviation ($\overline{x} \pm 2\sigma$) (e.g. Ghosh et al., 2009; Ramola et al., 2008; Oh and Kim, 2015). The concentration of residual radon exceeding the defined threshold ($\overline{x} \pm 2\sigma$) prior to the seismic activity can be considered as a pre-earthquake radon anomaly (Fu et al., 2017a). Moreover, the anomaly selection criteria adopted in this current study has a confidence interval of 95% (Gregoric et al., 2011). In addition to the above, analysis of residual radon instead of raw radon also increases the confidence level for identification of a pre-earthquake anomaly (Arora et al., 2017).

4. Results

4.1. Geochemical analysis of soil samples

Geochemical analysis of soil samples reveals some key information relating to the variability of radon concentration and soil characteristics in order to estimate radon potential. Spectroscopic measurements

Table 2
Activity concentrations of major radionuclides are expressed in Bq/kg at 95% confidence interval.

Isotope	Mean (Bq/kg)	SD (Bq/kg)	%SD
^{226}Ra	32.69	3.13	9.58
^{214}Pb	31.52	3.11	9.86
^{40}K	389	22	5.74

Table 3
Concentration of radionuclides expressed in Bq/kg for dry soil samples compared with international standard values.

Isotope	Observed (Bq/kg)	Reported (Bq/kg)
^{228}Ac	57.9 ± 4.8	57.6 ± 2.5
^{214}Bi	67.3 ± 6.3	67.0 ± 2.3
^{137}Cs	1493 ± 73	1450 ± 73
^{40}K	638 ± 51	636 ± 33
^{212}Pb	57.9 ± 1.7	57.9 ± 2.9
^{214}Pb	71.4 ± 6.2	71.1 ± 2.3
^{234}Th	127.3 ± 7.6	127.0 ± 7.1

confirm the presence of ^{226}Ra, ^{232}Th and ^{40}K with a mean value of 32.69 (Bq/kg), 31.52 (Bq/kg) and 389 (Bq/kg) and standard deviation of 3.13 (Bq/kg), 3.11 (Bq/kg) and 22 (Bq/kg) respectively (Table 2). Besides this, other radionuclides are also observed and compared with reported values in Table 3. Observed concentrations of naturally occurring radionuclides in the soil samples are within the normal range and any enhancement in radon concentration is not related to them but to some external factors (i.e. geodynamic activity or meteorological effects). In addition, other soil properties such as pH (8.1), conductivity (41.0 μS/cm) and soil moisture content (0.15%) were also measured.

4.2. Soil radon and meteorological parameters

The temporal variability of soil radon influenced by meteorological parameters (T, P and rH) of the soil and atmosphere are critically analyzed and compared. These parameters are recorded in the soil by a radon monitor and in the air by a meteorological station installed by PMD near the monitoring site. At the first stage, a comparison between soil and atmospheric pressure fluctuations was performed (Fig. 2a–b). The atmospheric pressure ranges from 936 to 964 mbar with an average value of 952 mbar. While, the pressure values for soil gas show almost similar trend with a slight difference in range (924–953 mbar) and average value (941 mbar).

At the second stage, a comparison between humidity and temperature measured by soil and atmospheric monitors respectively was performed (Fig. 2c–d). The atmospheric humidity ranges from 58% to 98% with an average value of 88%. The atmospheric temperature corresponding to humidity shows an inverse trend, within a range of 11.2–37.7 °C with an average value of 25.8 °C. Soil humidity and temperature demonstrate analogous behavior, as presented in Fig. 2c, with a range of 44–96% for soil humidity and 4.7–38.8 °C for soil temperature. Furthermore, the daily and cumulative behavior of rainfall data for the selected time window was also examined to analyze their influence on the temporal variability of radon (Fig. 2e). The months of July–August 2014 and February 2015 are marked as periods of highest rain-fall showing a surge in cumulative and daily rain-fall.

4.3. Deterministic analysis

A deterministic analysis (fractal method) of radon data along with meteorological parameters has been performed to estimate the degree of chaotic behavior and long-range discrepancies in the time series by using a mathematical quantity known as the Hurst exponent (H). H is estimated for the whole data set via Equation (6) and it categorizes the

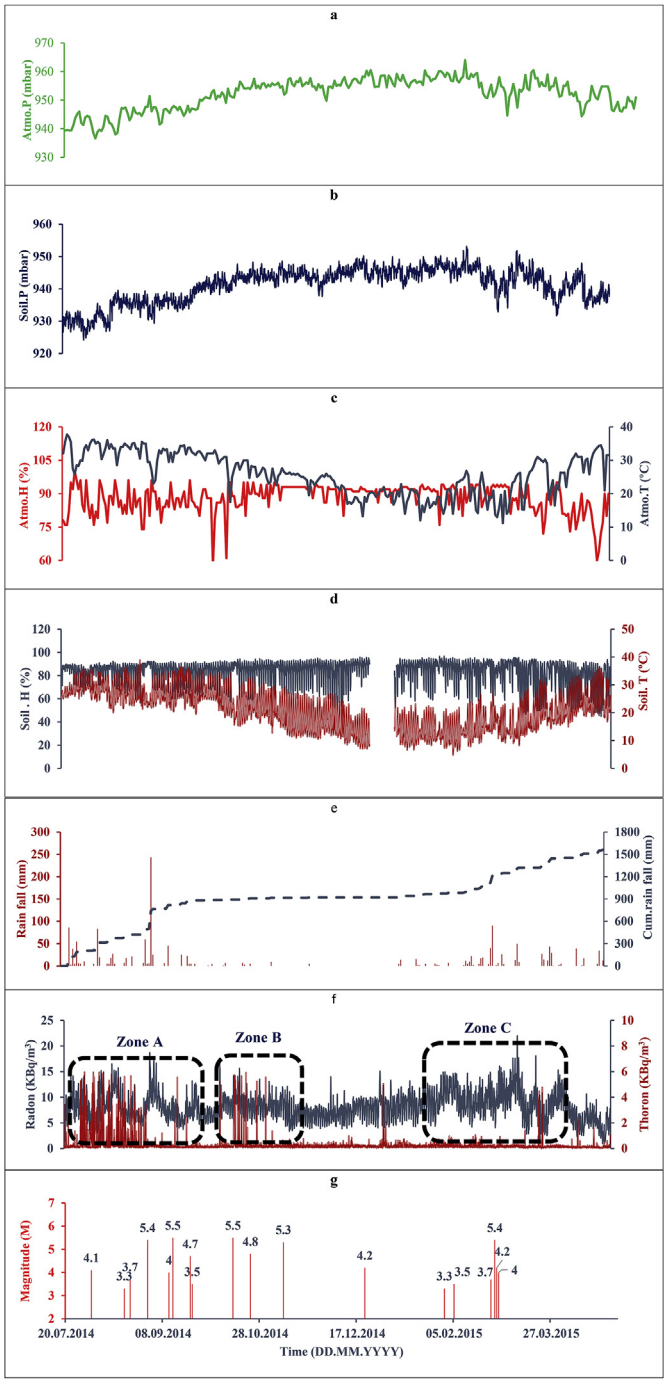

Fig. 2. The time series plot of soil radon, meteorological parameters (soil and atmosphere) and earthquakes is presented here form July 25, 2014 to April 30, 2015. Fig. 2a and b presents a comparison between atmospheric and soil pressure. Fig. 2c and d illustrate that the humidity and temperature depict an inverse relationship among them for soil and atmospheric possible due to rainfall presented in Fig. 2e. Cumulative rainfall data indicate heavy rain fall for the months of July, August and September whereas relatively straight line from September to March show very minimal rainfall. Temporal change of radon further divided in three zone (Zone A, zone B and Zone C) based on the observed abnormalities of radon and thoron presented in 3e. The detailed analysis of these identified anomalous zone are presented in Fig. 4–6. Besides this, some anomalous peaks in thoron also identified prior to earthquake events. Population of earthquake events (g) corresponding to the selected anomalous zone (e) is high.

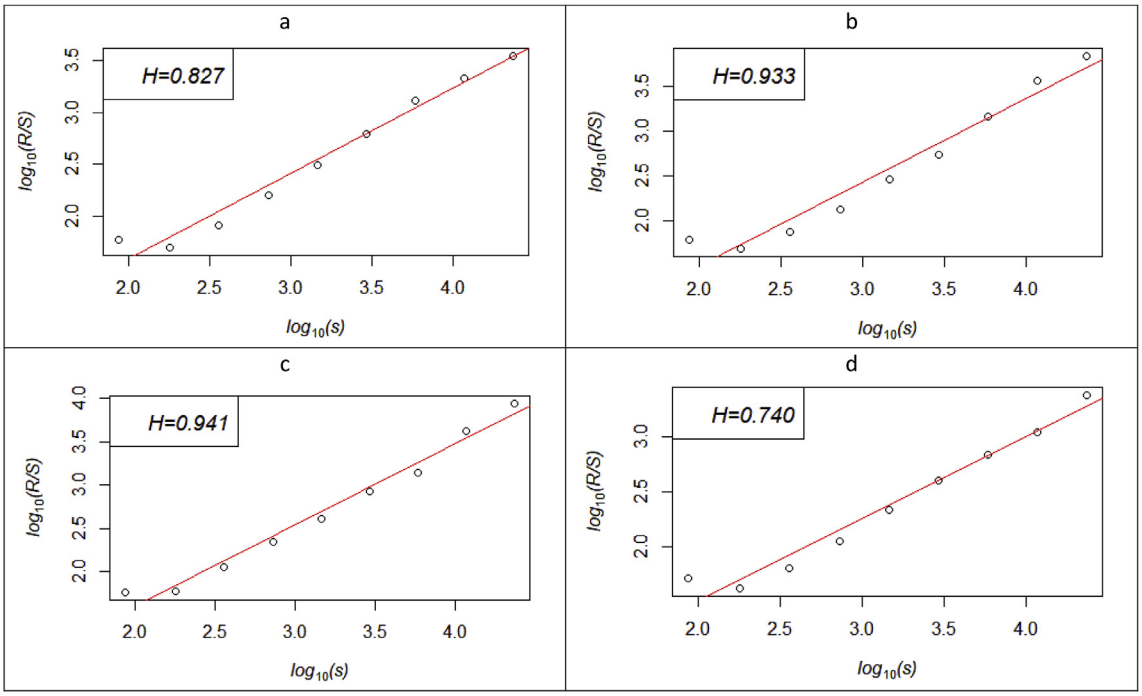

Fig. 3. The R/S analysis results for selected time series of soil radon and meteorological parameters. (a) Hurst exponent estimated for whole data set of radon showing a persistent behavior. For meteorological parameters such as (b) temperature; (c) pressure and (d) humidity, Hurst exponent is found to be within the range of $0.5 \leq H \leq 1$.

dataset by its deviation as persistent, anti-persistent or random in chaotic regime as discussed in section 3.2.1. Our radon data lie in the persistent category with a H value of 0.827 (Fig. 3a). Furthermore, the H value for meteorological parameters are 0.933 (T), 0.941 (P) and 0.740 (rH) respectively (Fig. 3b-d).

4.4. Recognition of anomalous radon concentration and its tectonic implications

The times series analysis of soil radon presented in Fig. 23e shows anomalous radon/thoron peaks along with accompanying meteorological parameters of the soil and atmosphere. Such an anomalous variability in radon values can possibly be correlated with tectonic activity (i.e. earthquakes shown in Fig. 2f) during the selected time window. For detailed investigation of anomalous soil radon and their tectonic implications, the selected time window was divided into three zones (Zones A, B and C). All zones were critically analyzed and results are presented in Figs. 4–6 along with corresponding earthquake events. Before correlating radon variability with seismic activity, a 7 days rolling average was applied to the radon time series to eliminate diurnal and short term effects. The variability of raw radon data (hourly variation), the trend line (daily moving average) and the rolling average (7 days moving) show distinct and robust peaks (Fig. 4a). To recognize anomalous peaks associated with an impending earthquake event, a statistical criterion discussed in section 3.2 was applied on residual radon computed via Equation (2) (Fig. 4b).

The first notable anomalous zone (Zone A) ranges from July 24 to September 25 2014 as presented in Fig. 4. Earthquake events for the selected time window (July 24 2014 to September 25 2014) recorded by local and global seismic networks are presented in Fig. 4c. During the selected time period of Zone A, 8 seismic events are reported with their magnitude ranging from 3.3 to 5.5. The residual radon values surpass the statistically bound 2 days prior to a shallow focused (35 km) and moderate (M 4.1) earthquake having $R_E < 1.5R_D$. The corresponding anomalous variation of the raw radon, trend line and rolling average shown by the vertical column in Fig. 4 can also be observed. For the two events of low magnitude (3.3, 3.7) during the selected time period of Zone A, the residual radon value was observed to be within the statistically bound area. However, the raw and trend radon data show anomalous peaks almost 5–10 days prior to these events. The absence of residual anomalous peaks for these events can be attributed to higher R_E/R_D values as shown in Table 1.

A very prominent anomalous peak of residual radon surpassing the statistical bound can be observed for an earthquake event of M 5.4. The threshold of statistical bound is crossed almost 3 days prior to this particular event. The raw radon and trend line corresponding to this particular event reveal a plausible correlation in the form of anomalous peaks. Anomalous behavior of residual radon is found to be absent for two earthquake events (M 4, 5.5) reported on September 11–13 2014. For these events, only the raw radon data shows an increase with low amplitude. Again this can be attributed to higher R_E/R_D values given in Table 1. The Zone A ends with a moderate amplitude residual and a high amplitude raw/trend radon anomaly 4 days prior to the two events of magnitude 4.7 and 3.5 (Fig. 4).

A detailed investigation of the second notable anomalous zone (Zone B; Fig. 2f) ranging from September 25 2014 to November 15 2014 is presented in Fig. 5. The first anomalous peak of residual radon surpassing the statistical bound in Zone B is observed on October 01 2014, preceding a seismic event with a magnitude of 5.5. The corresponding raw and trend line radon concentrations also show inconsistent behavior prior to this particular event. The second anomalous residual radon peak crossing the statistical threshold can be observed 8 days prior to an earthquake event of magnitude 4.8. Again for this event, an inconsistent change in the raw and trend line radon concentration can be observed. Residual and raw radon concentrations fail to capture any anomalous behavior for an event occurring on November 09 2014, having magnitude 5.3 due to higher R_E/R_D value.

The third notable anomalous zone (Zone C) ranging from December 20 2014 to March 15 2015 is presented in Fig. 6. The temporal variability of residual and raw radon is unable to exhibit any precursory signals associated with two low magnitude events recorded on January 31 and February 05 2015, possibly due to high R_E/R_D values (Table 1;

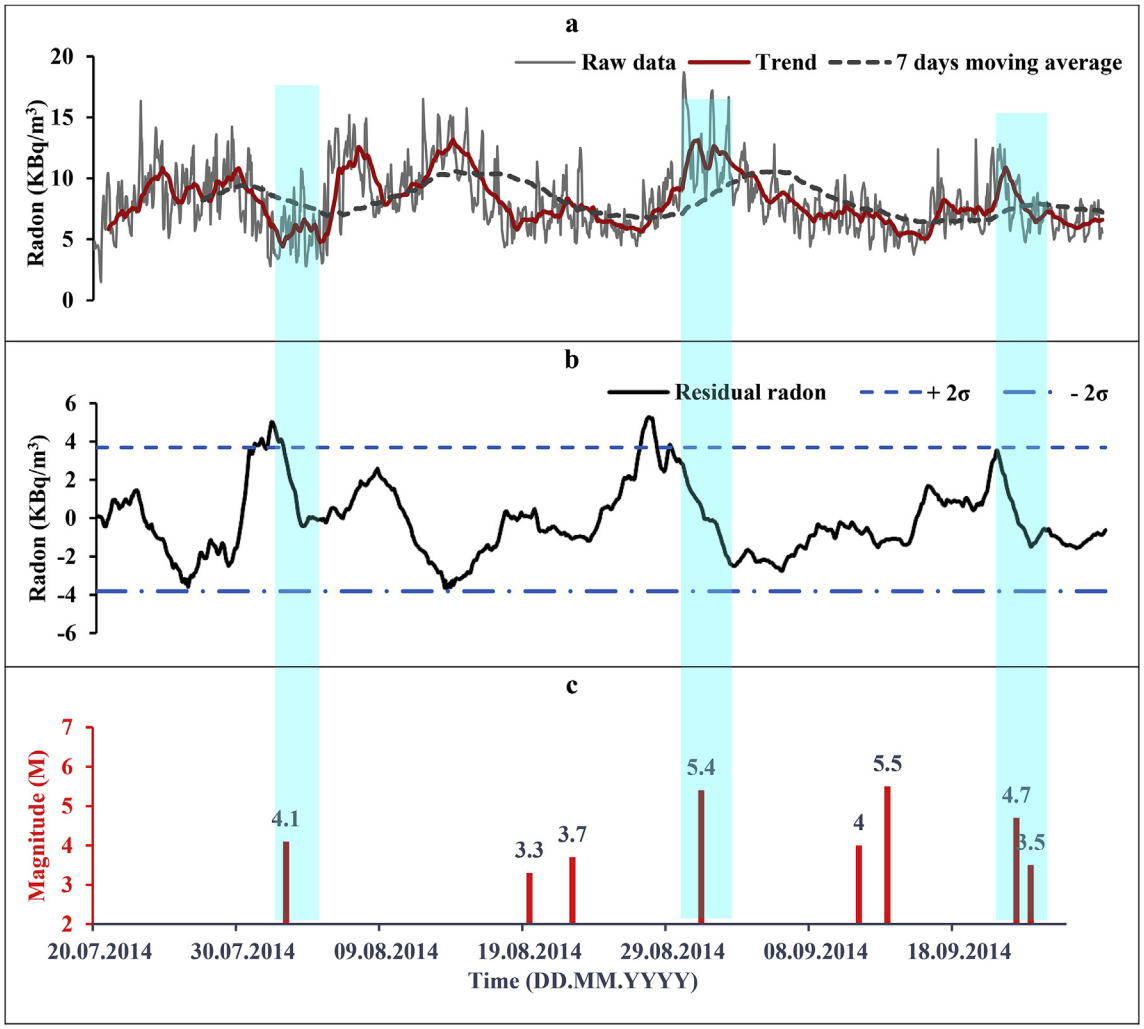

Fig. 4. A detailed statistical analysis of anomalous Zone A from July 24, 2014 to September 25, 2014 (a) Temporal variation of raw soil radon along with trend (24 h average) and moving average (7 days) reveals some anomalous fluctuations of radon. The residual radon concentration computed via Eq. 9 is plotted in (b) showing three abnormal peaks overpassing the threshold (± 2σ) of anomaly selection. Vertical light green colour bars show a linkage between earthquakes, residual, raw, trend and 7 days rolling average of radon. (For interpretation of the references to colour in this figure legend, the reader is referred to the Web version of this article.)

Fig. 6a). A comparative analysis of raw, trend and 7 day rolling average radon data reveal 2 extreme peaks observed (February 8–15, 2015) nearly 10–12 days prior to the 4 recorded earthquake events having magnitudes of 3.7, 5.4, 4 and 4.2 (Fig. 6c). The corresponding residual radon concentration shows a rapid rise/fall trend before these events. In particular the residual radon exceeds the threshold of ± 2σ almost 12–15 days prior to the occurrence of these events. Furthermore, over the entire time series multiple thoron peaks are also observed prior to numerous reported events despite its shorter half-life.

5. Discussion

The present study has analyzed the association of radon with its controlling factors in the context of pre- co- and post-seismic processes. Numerous studies suggest analysis of all potential controlling factors (soil geochemistry and meteorological parameters) for radon need to carried out prior to attempting any correlation with geodynamic activity. In general, the temporal variability of soil radon flux associated with the seismo-tectonically driven forces has been suggested by numerous researchers in the last few decades (Planinic et al., 2004; Fujiyoshi et al., 2006; Choubey et al., 2007; Ghosh et al., 2009; Vaupotic et al., 2010; Tarakçı et al., 2014; Woit, 2015; Jilani et al., 2017; Singh et al., 2017). Radon measurements have been carried out in different media (e.g. water, soil and air) within the context of earthquake forecasting (Gosh et al., 2009; Cicerone et al., 2009; Woith, 2015; Riggio and Santulin, 2015; WHuang et al., 2017).

The first controlling factor is the radionuclides concentration (uranium, radium and potassium) that may be spatially associated with soil radon anomalies (Sroor et al., 2001; Singh et al., 2005a; Baykara and Dogru, 2006; Kurnaz et al., 2007; Vinson et al., 2009; Sharma et al., 2016; Forkapic et al., 2017). There is a general lack of consensus on the extent to which soil radionuclide concentration influences soil radon. For instance, Sroor et al. (2001) analyzed soil samples to explore the relationship between natural radioactivity and radon exhalation rate of soil in southern Egypt. They concluded that the radon exhalation rate and uranium concentration coincide with each other for the same soil sample. Singh et al. (2005a) determine the concentration of naturally occurring radionuclides in soil samples from Punjab and Himachal Pradesh, India. They reported the activity concentration of ^{226}Ra (18.22–90.30 Bq/kg) and ^{232}Th (34.80–124.68 Bq/kg) in soil is higher and for ^{40}K (80.42–181.41 Bq/kg) is lower than the world average. Additionally, Appleton et al. (2008) also reported a good agreement between radon and soil geochemical analysis using different multivariate regression correlations. On the other hand, Vinson et al. (2009) explored the relationship between radium content and radon occurrence from fractured crystalline rocks in North Carolina, USA. They

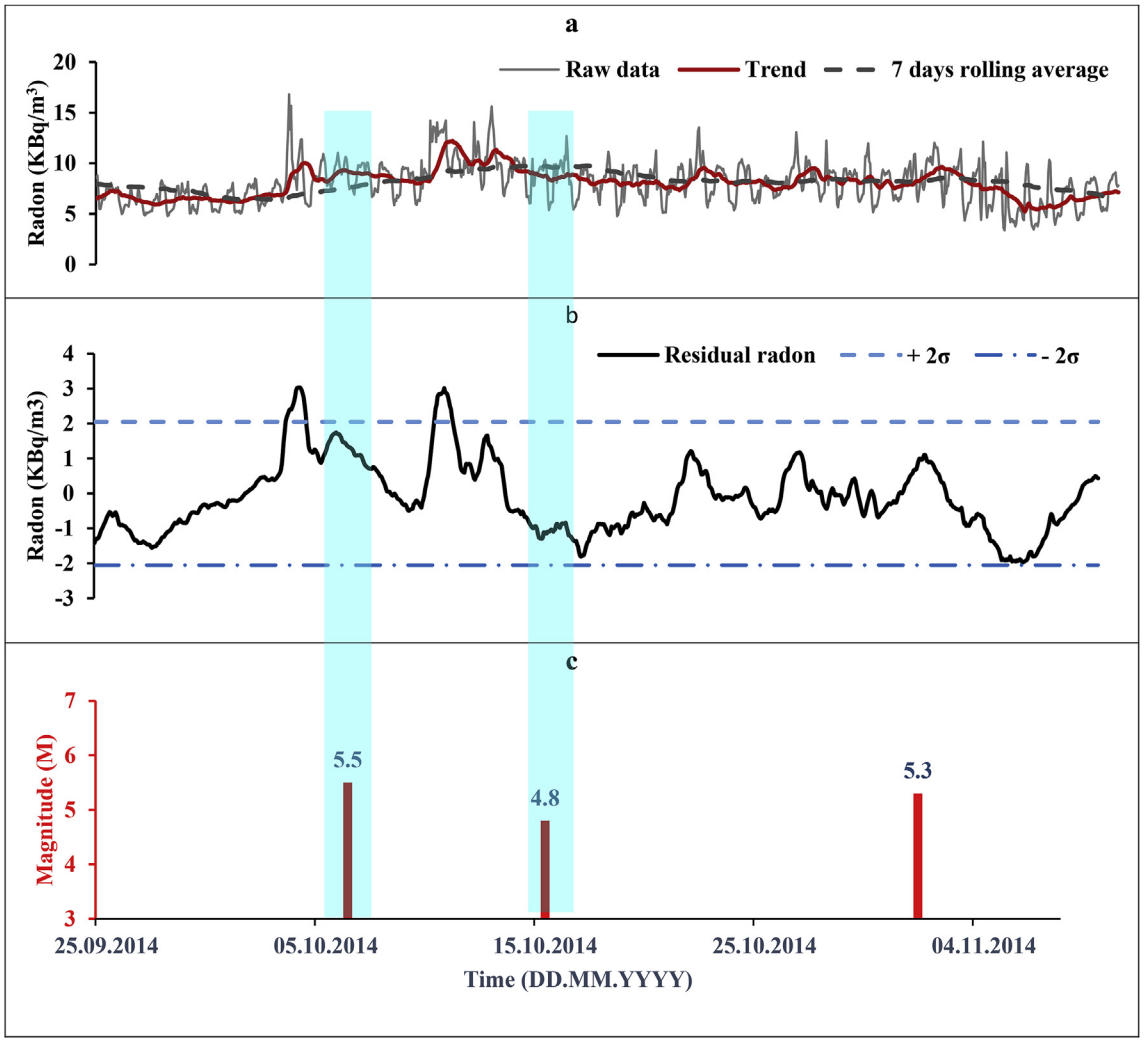

Fig. 5. A detailed investigation of second notable radon anomalous zone (Zone B) for a time interval of September 25, 2014 to Nov 15, 2015 is presented here. Raw radon data show multiple high amplitude peaks in Fig. 2f prior to recorded earthquake events. The residual radon concentration show two peak overpasses the threshold of anomaly selection and followed by two earthquakes. The light green vertical bar shows the linkage between the peaks of raw, trend, residual radon and earthquakes. (For interpretation of the references to colour in this figure legend, the reader is referred to the Web version of this article.)

found that the content of radionuclides in the soil samples collected around the monitoring site is minimal and their effect on radon enhancement is insignificant.

Sharma et al. (2016) concluded that it is hard to estimate the radon concentration from ^{226}Ra content as it depends on many other factors. For example, Faheem and Matiullah (2008) explored that the radon exhalation rate and moisture content have a direct relation up to a certain limit and then radon exhibits a decreasing trend with a further increase in moisture content. Forkapic et al. (2017) provides values of linear correlation coefficients by incorporating all possible input variables that can affect the radon concentration. They suggested that the radon level greatly depends on the concentration of ^{226}Ra and ^{232}Th as compared to other input variables such as pH, ^{238}U, ^{40}K and ^{137}Cs. In current study, the activity concentrations of major radionuclides observed in soil samples are found to be in accordance with some investigations as discussed earlier. For example, the low activity concentration of 226Ra (32.69Bq/kg) does not suggests any apparent correlation with radon level. It can be concluded that 226Ra is not a prominent factor controlling soil radon levels for this particular case. Overall, the results of radionuclides summarized in Tables 2 and 3 are found to be within the typical range and for the studied area their effect on radon enhancement is insignificant.

The second important factor affecting soil radon concentration are meteorological parameters. It is often difficult to discriminate an anomaly caused solely by meteorological parameters or seismic activity, therefore the meteorological effect should be taken into consideration (Oh and Kim, 2015; Fu et al., 2017a). In this regard, analysis of meteorological parameters prior to correlating the radon with geodynamic activity is of utmost importance (Zafrir et al., 2016). Numerous researchers have worked to establish relationships between radon variability and meteorological parameters (Iakovleva and Ryzhakova, 2003; Singh et al., 2017; Oh and Kim, 2015; Jilani et al., 2017). For example, Singh et al. (2017) monitored the soil radon level along with key meteorological parameters in some area of Northern Punjab, India. They concluded that a negative correlation exists between radon and temperature (−0.4), while a positive correlation exists between pressure (0.2) and humidity (0.4). Contrary to the above, Iakovleva and Ryzhakova (2003) estimated a positive correlation for soil temperature and radon (0.752) whereas, negative correlation for atmospheric pressure (−0.861) and humidity (−0.555) for the city of Tomsk (West Siberia, Russia).

In the present study, the variability of meteorological parameters in soil and air is monitored for the selected time window (Fig. 2). The temporal variability of meteorological parameters of soil and atmosphere reveals a symmetrical behavior with a slight variation in their amplitude. For example, an analogy exists among atmospheric and soil

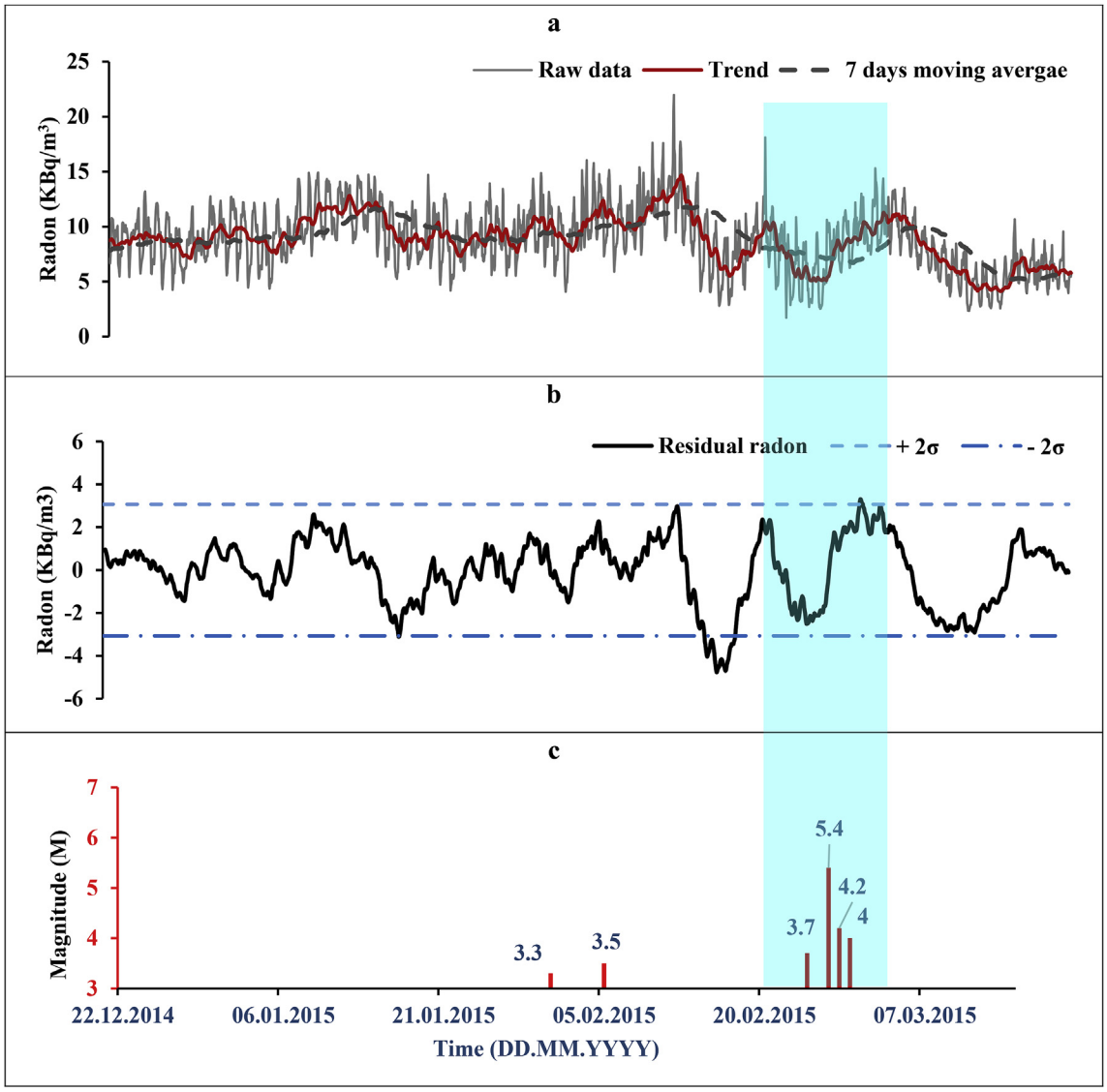

Fig. 6. A detailed investigation of temporal variability of notable anomalous zone (Zone C) for a time window of Dec 20, 2014 to March 15, 2015 is presented here. Over a selected time window abnormal increasing decreasing pattern of raw, trend and residual radon concentration followed by a series of seismic events were observed. Residual radon concentration overpasses the threshold prior to recorded earthquakes indicated by light green vertical column. (For interpretation of the references to colour in this figure legend, the reader is referred to the Web version of this article.)

pressure value with slight variation (Fig. 2 a–b). However, the variability of soil radon inflicted by pressure is found to be least significant due to its low correlation coefficient (0.05).

The relationship between humidity and temperature is presented in Fig. 2c–d showing an analogous inverse trend. A negative correlation (−0.268) exists between temperature and radon while, a positive correlation (0.374) exist between humidity and radon during the selected time interval. Fujiyoshi et al. (2006) and Arora et al. (2017) also reported a direct relationship between humidity and radon and an inverse relationship for temperature possibly due to an increase of water content which may holds higher concentration of radon progenies (Singh et al., 2005b).

By comparing radon with rainfall data (Fig. 2e–f), it is observed that at the onset of rain, radon shows a surge with a time lag, possibly due to the entrapment of soil radon (Arora et al., 2017). As expected, the frequency of rainfall was found to be higher for the months of July–August 2015 and lower from November–January 2014 (Fig. 2e). A very clear relationship can be observed between the asymmetrical trend of humidity and temperature values presented in Fig. 2c and rainfall data (Fig. 2e). Extreme values of humidity and temperature from July to September 2014 are possibly due to the highest rainfall values for the corresponding time interval and vice versa. Overall, the comparison presented in Fig. 2c–d suggests that a temporal progression of humidity/temperature is dependent on each other for soil and atmosphere. It is worth mentioning that the low correlation among radon and meteorological parameters reveals that radon enhancement is possibly related with some others external factors (i.e. seismic activity) recorded during the selected time window.

The third important factor is the temporal analysis of radon along with its controlling parameters to determine the degree of chaotic behavior and examine the dynamics of radon concentration reported in numerous studies (Pausch et al., 1999; Planinic et al., 2004; Barbosa et al., 2007; Tatli, 2015). The estimation of a fractal element for radon time series facilitates exploring the underlying dynamics of a physical system such as seismic activity (Barman et al., 2015). Overall, a wide range of values for H are reported in many studies for radon and meteorological parameters. This range mainly depends on the methodology adopted for monitoring and quality of the data (Pausch et al., 1999; Planinic et al., 2004; Barbosa et al., 2007; Nikolopoulos et al., 2014; Gkarlaouni et al., 2017). For example, Planinic et al. (2004)

calculate the chaotic behavior of radon along with pressure and temperature in different environments. They concluded that environmental parameters exhibit a persistent trend ($H > 0.5$) while, the behavior of radon is anti-persistent ($H < 0.5$) i.e. a decreasing trend in the past implies a probable increase in future and vice versa. On the contrary, different values of H for radon have been obtained in many studies e.g., Planinic et al. (2004). In current study, the fractal dimensions of radon time series exhibit characteristics of deterministic chaos with $0.5 < H < 1$ i.e. persistent trend. Furthermore, the persistence of controlling meteorological parameters of radon time series attests to their mutual dependency. In summary, the H computed in the current study exhibits a persistent trend for radon and its accompanying meteorological parameters. Therefore, no chaotic behavior can be expected in our radon data, consistent with some prior observations as discussed earlier.

Analyses of all the above three factors intend to explore the temporal reconnaissance of soil radon within the context of earthquake forecasting. The main rationale behind this temporal reconnaissance of radon is the tectonic stresses associated with the impending earthquake event (Walia et al., 2013; Woith, 2015; Zafrir et al., 2016; Arora et al., 2017). In this regard, Pulinets and Ouzounov (2011) proposed a physical mechanism that systematically explain the synergy between pre-earthquake signals and seismic activity is proposed by Pulinets and Ouzounov (2011) in the form of Lithosphere–Atmosphere–Ionosphere Coupling (LAIC) model. According to LAIC model, the relative movement of the tectonic blocks increasing the stress level which leads to opening of micro-fractures in the impending focal zone facilitating the emanation of soil gases that can serve as earthquake precursors. However, there is a lack of universally accepted model that conceivably demonstrate the precursory nature of radon anomalies (Woith, 2015).

The current study encompasses the significance of residual signal processing techniques which diminish the regular frequent effect of data recording. A very distinct feature of this technique is linked with the reduction of any kind of random noise related to regular frequent effects of data recording (Fu et al., 2017; Arora et al., 2017). Furthermore, the anomaly selection criteria ($\overline{x} \pm 2\sigma$) applied on residual radon concentration helps in identification on earthquake related signals by lowering the probability of false anomalies (Hartmann and Levy, 2005; Fu et al., 2017a). The statistical criterion of ($\overline{x} \pm 2\sigma$), means that we have a confidence interval of 95% for identification of a radon anomaly. In other words, there is only a 5% probability that a spike overpassing this criterion in radon data can exist (Planinic et al., 2001).

The results of the present investigation inferred interplay between the magnitude of an earthquake event, the location of a radon monitoring site and the distance from the event epicenter (Inan et al., 2008). For example, radon variations fail to register any anomalous change associated with a distant earthquake event of Zone A recorded on September 13 2014, despite of its high magnitude ($M > 4$). On contrary, radon variation seems to be more responsive for impending earthquake events of low magnitude and low R_E/R_D values belonging to Zone A. Likewise, the results of Zone B further endorse the presence of radon anomalies around the time of selected earthquakes with high magnitude and low R_E/R_D value. The Zone C presents a scenario of anomalous radon signals possibly caused by an earthquake swarms of small events. In this case, the largest earthquake ($M = 5.4$; Fig. 6) is assumed to precede the anomaly as reported in earlier investigations (Hartmann and Levy, 2005). It is worth mentioning that the radon anomaly associated with this swarm of earthquakes also fulfills the superposition of pre- co- and post-seismic signals.

In particular, notable anomalous peaks of residual radon are identified prior earthquake events of magnitude > 4.0 and low R_E/R_D values. Moreover, the absence of anomalous peaks prior to a few earthquake events in the selected time window can be attributed to their low magnitude and high R_E/R_D values. Besides this, the temporal variability of thoron also reveals few upsurges around the time of a few earthquake events during the selected time window, suggesting a change in depth of the predominant source of soil radon. However, least preference is given to thoron in the context of earthquake forecasting due to its relatively shorter half-life (55.6 s).

The present investigation reveals that the results obtained in this study are consistent with the results reported by Jilani et al. (2017) and Barkat et al. (2017) at other radon monitoring sites within this region.

6. Conclusions

In the current study, a systematic monitoring of soil radon along with key meteorological parameters is conducted within the context of earthquake forecasting. In particular, before correlating fluctuations of soil radon with impending earthquakes, we have performed: (1) a geochemical analysis of soil around the monitoring site, and (2) statistical (Hurst) analysis of soil radon and meteorological parameters. Our results suggest a clear relationship between the variability of soil radon and seismic events. The main results of this study are summarized as:

a) Geochemical analyses reveal that the content of radionuclides in the soil is comparable to standard values. This suggest that any enhancement in radon is not related with the occurrence of natural radionuclides as well as other soil properties such as soil moisture content, pH, conductivity etc.
b) The deterministic analysis of radon and meteorological parameters reveals a positively auto-correlated persistent long-memory trend indicating that past trend of selected data is more likely to be continued than to be inverted in the future.
c) The low correlation coefficients among radon and meteorological parameters disclose that any anomalous enhancement of radon is not attributed to a meteorological change.
d) The statistical analysis (residual signal processing technique; $\overline{x} \pm 2\sigma$) of soil radon variability reveals the presence of three periods (Zones A, B and C) of significant radon enhancements. In every period, notable peaks of residual radon were identified with impending earthquake activity. It is worth mentioning that the current statistical approach fails to capture any anomalous change associated with the earthquakes of low magnitude and high R_E/R_D value. Inclusively, the existence of such a significant correlation between the results observed for different monitoring stations endorses the use of a dense network of radon monitoring for earthquake prediction studies.

Acknowledgment

The authors wish to acknowledge two anonymous reviewers for the improvement of manuscript by their constructive remarks. Gratitude is also extended to Michael Kersten for his editorial assistance. Dr. Aamir Ali would like to thank the Department of Earth Sciences, Quaid-i-Azam University, Islamabad, Pakistan for providing the basic requirements to complete this work. Mr. Adnan Barkat is thankful to all co-workers at Centre for Earthquake Studies for their valuable suggestions. All the authors are thankful to Pakistan Meteorological Department for providing the atmospheric meteorological data.

References

Ali, Z., Qaisar, M., Mahmood, T., Shah, M.A., Iqbal, T., Serva, L., Burton, P.W., 2009. The Muzaffarabad, Pakistan, earthquake of 8 October 2005: surface faulting, environmental effects and macroseismic intensity. Geological Society, London, Special Publications 316 (1), 155–172. https://doi.org/10.1144/SP316.9.

Appleton, J.D., Miles, J.C.H., Green, B.M.R., Larmour, R., 2008. Pilot study of the application of Tellus airborne radiometric and soil geochemical data for radon mapping. J. Environ. Radioact. 99 (10), 1687–1697. https://doi.org/10.1016/j.jenvrad.2008.03.011.

Arora, B.R., Kumar, A., Walia, V., Yang, T.F., Fu, C.C., Liu, T.K., Chen, C.H., 2017. Assesment of the response of the meteorological/hydrological parameters on the soil gas radon emission at Hsinchu, northern Taiwan: a prerequisite to identify

earthquake precursors. J. Asian Earth Sci. 149, 49–63. https://doi.org/10.1016/j.jseaes.2017.06.033.
Asim, K.M., Martínez-Álvarez, F., Basit, A., Iqbal, T., 2017. Earthquake magnitude prediction in Hindukush region using machine learning techniques. Nat. Hazards 85 (1), 471–486. https://doi.org/10.1007/s11069-016-2579-3.
Awais, M., Barkat, A., Ali, A., Rehman, K., Zafar, W.A., Iqbal, T., 2017. Satellite thermal IR and atmospheric radon anomalies associated with the Haripur earthquake (Oct 2010; Mw 5.2), Pakistan. Adv. Space Res. https://doi.org/10.1016/j.asr.2017.08.034.
Barbosa, S.M., Steinitz, G., Piatibratova, O., Silva, M.E., Lago, P., 2007. Radon variability at the Elat granite, Israel: heteroscedasticity and nonlinearity. Geophys. Res. Lett. 34 (15). https://doi.org/10.1029/2007GL030065.
Barkat, A., Ali, A., Siddique, N., Alam, A., Wasim, M., Iqbal, T., 2017. Radon as an earthquake precursor in and around northern Pakistan: a case study. Geochem. J. 51 (4), 337–346. http://doi.org/10.2343/geochemj.2.0473.
Barkat, A., Ali, A., Rehman, K., Awais, M., Tariq, M.A., Ahmed, J., Iqbal, T., 2018. Multi-precursory analysis of phalla earthquake (July 2015; Mw 5.1) near Islamabad, Pakistan. Pure Appl. Geophys. 1–16. https://doi.org/10.1007/s00024-018-1927-5.
Barman, C., Chaudhuri, H., Deb, A., Ghose, D., Sinha, B., 2015. The essence of multifractal detrended fluctuation technique to explore the dynamics of soil radon precursor for earthquakes. Nat. Hazards 78 (2), 855–877. https://doi.org/10.1007/s11069-015-1747-1.
Baykara, O., Dogru, M., 2006. Measurements of radon and uranium concentration in water and soil samples from East Anatolian Active Fault Systems (Turkey). Radiat. Meas. 41 (3), 362–367. https://doi.org/10.1016/j.radmeas.2005.06.016.
Bem, E.M., Bem, H., Wieczorkowski, P., 1998. Studies of radionuclide concentrations in surface soil in and around fly ash disposal sites. Sci. Total Environ. 220 (2), 215–222. https://doi.org/10.1016/S0048-9697(98)00258-7.
Choubey, V.M., Mukherjee, P.K., Bajwa, B.S., Walia, V., 2007. Geological and tectonic influence on water–soil–radon relationship in Mandi–Manali area, Himachal Himalaya. Environ. Geol. 52 (6), 1163–1171. https://doi.org/10.1007/s00254-006-0553-1.
Cicerone, R.D., Ebel, J.E., Britton, J., 2009. A systematic compilation of earthquake precursors. Tectonophysics 476 (3), 371–396. https://doi.org/10.1016/j.tecto.2009.06.008ce.
Dobrovolsky, I.P., Zubkov, S.I., Miachkin, V.I., 1979. Estimation of the size of earthquake preparation zones. Pure Appl. Geophys. 117 (5), 1025–1044. https://doi.org/10.1007/BF00876083.
Faheem, M., Matiullah, 2008. Radon exhalation and its dependence on moisture content from samples of soil and building materials. Radiat. Meas. 43 (8), 1458–1462. https://doi.org/10.1016/j.radmeas.2008.02.023.
Faisal, S., Larson, K.P., Cottle, J.M., Lamming, J., 2014. Building the Hindu Kush: monazite records of terrane accretion, plutonism and the evolution of the Himalaya–Karakoram–Tibet orogen. Terra. Nova 26 (5), 395–401. https://doi.org/10.1111/ter.12112.
Forkapic, S., Maletić, D., Vasin, J., Bikit, K., Mrdja, D., Bikit, I., Banjanac, R., 2017. Correlation analysis of the natural radionuclides in soil and indoor radon in Vojvodina, Province of Serbia. J. Environ. Radioact. 166, 403–411. https://doi.org/10.1016/j.jenvrad.2016.07.026.
Fu, C.C., Walia, V., Yang, T.F., Lee, L.C., Liu, T.K., Chen, C.H., Wen, K.L., 2017a. Pre-seismic anomalies in soil-gas radon associated with 2016 M 6. 6 Meinong earthquake, Southern Taiwan. Terrestrial Atmospheric and Oceanic Science Journal 28 (5), 787–798. https://doi.org/10.3319/TAO.2017.03.22.01.
Fu, C.C., Yang, T.F., Chen, C.H., Lee, L.C., Wu, Y.M., Liu, T.K., Lai, T.H., 2017b. Spatial and temporal anomalies of soil gas in northern Taiwan and its tectonic and seismic implications. J. Asian Earth Sci. 149, 67–77. https://doi.org/10.1016/j.jseaes.2017.02.032.
Fujiyoshi, R., Sakamoto, K., Imanishi, T., Sumiyoshi, T., Sawamura, S., Vaupotic, J., Kobal, I., 2006. Meteorological parameters contributing to variability in 222 Rn activity concentrations in soil gas at a site in Sapporo, Japan. Sci. Total Environ. 370 (1), 224–234. https://doi.org/10.1016/j.scitotenv.2006.07.007.
Ghosh, D., Deb, A., Sengupta, R., 2009. Anomalous radon emission as precursor of earthquake. J. Appl. Geophys. 69 (2), 67–81. https://doi.org/10.1016/j.jappgeo.2009.06.001.
Gkarlaouni, C., Lasocki, S., Papadimitriou, E., George, T., 2017. Hurst analysis of seismicity in Corinth rift and Mygdonia graben (Greece). Chaos, Solit. Fractals 96, 30–42. https://doi.org/10.1016/j.chaos.2017.01.001.
Gregoric, A., Zmazek, B., Dzeroski, S., Torkar, D., Vaupotic, J., 2011. Radon as an earthquake precursor-methods for detecting anomalies. Earthquake Research and Analysis Statistical Studies, Observations and Planning. InTech.
Hartmann, J., Levy, J.K., 2005. Hydrogeological and gas-geochemical earthquake precursors–A review for application. Nat. Hazards 34 (3), 279–304. https://doi.org/10.1007/s11069-004-2072-2.
Huang, F., Li, M., Ma, Y., Han, Y., Tian, L., Yan, W., Li, X., 2017. Studies on earthquake precursors in China: A review for recent 50 years. Geodesy Geodyn. 8 (1), 1–12. https://doi.org/10.1016/j.geog.2016.12.002.
akovleva, V.S., Ryzhakova, N.K., 2003. Spatial and temporal variations of radon concentration in soil air. Radiat. Meas. 36 (1–6), 385–388. https://doi.org/10.1016/S1350-4487(03)00156-2.
Inan, S., Akgül, T., Seyis, C., Saatçılar, R., Baykut, S., Ergintav, S., Baş, M., 2008. Geochemical monitoring in the Marmara region (NW Turkey): a search for precursors of seismic activity. J. Geophys. Res.: Solid Earth 113 (B3). https://doi.org/10.1029/2007JB005206.
Jilani, Z., Mehmood, T., Alam, A., Awais, M., Iqbal, T., 2017. Monitoring and descriptive analysis of radon in relation to seismic activity of Northern Pakistan. J. Environ. Radioact. 172, 43–51. https://doi.org/10.1016/j.jenvrad.2017.03.010.
Kazmi, A.H., Jan, M.Q., 1997. Geology and Tectonics of Pakistan. Graphic Publishers, Karachi, Pakistan.
Kearey, P., Klepeis, K.A., Vine, F.J., 2013. Global Tectonics. John Wiley and Sons, New York, USA.
Kikaj, D., Vaupotič, J., 2017. Parameters influence deviation of radon concentration from its typical diurnal pattern in the winter and summer season. Geologica Mecedonica 31 (2), 157–170.
Külahcı, F., Şen, Z., 2014. On the correction of spatial and statistical uncertainties in systematic measurements of ^{222}Rn for earthquake prediction. Surv. Geophys. 35 (2), 449–478. https://doi.org/10.1007/s10712-013-9273-8.
Kurnaz, A., Küçükömeroğlu, B., Keser, R., Okumusoglu, N.T., Korkmaz, F., Karahan, G., Çevik, U., 2007. Determination of radioactivity levels and hazards of soil and sediment samples in Fırtına Valley (Rize, Turkey). Appl. Radiat. Isot. 65 (11), 1281–1289. https://doi.org/10.1016/j.apradiso.2007.06.001.
Laskar, I., Phukon, P., Goswami, A.K., Chetry, G., Roy, U.C., 2011. A possible link between radon anomaly and earthquake. Geochem. J. 45 (6), 439–446. https://doi.org/10.2343/geochemj.1.0146.
Li, Y., Tan, W., Tan, K., Liu, Z., Xie, Y., 2016. Fractal and chaos analysis for dynamics of radon exhalation from uranium mill tailings. Fractals 24 (03), 1650029. https://doi.org/10.1142/S0218348X16500298.
Molnar, P., Tapponnier, P., 1975. Cenozoic tectonics of Asia: effects of a continental collision. Science 189 (4201), 419–426. https://doi.org/10.1126/science.189.4201.419.
Nikolopoulos, D., Petraki, E., Vogiannis, E., Chaldeos, Y., Yannakopoulos, P., Kottou, S., Stonham, J., 2014. Traces of self-organisation and long-range memory in variations of environmental radon in soil: comparative results from monitoring in Lesvos Island and Ileia (Greece). J. Radioanal. Nucl. Chem. 299 (1), 203–219. https://doi.org/10.1007/s10967-013-2764-8.
Oh, Y.H., Kim, G., 2015. A radon-thoron isotope pair as a reliable earthquake precursor. Sci. Rep. 5. https://doi.org/10.1038/srep13084.
Papastefanou, C., 2010. Variation of radon flux along active fault zones in association with earthquake occurrence. Radiat. Meas. 45 (8), 943–951. https://doi.org/10.1016/j.radmeas.2010.04.015.
Pausch, G., Bossew, P., Hofmann, W., Steger, F., 1999. Analysis of chaotic behavior of indoor radon concentrations. Proceedings of the Radon in the living Environment 37–51.
Planinić, J., Radolić, V., Lazanin, Ž., 2001. Temporal variations of radon in soil related to earthquakes. Appl. Radiat. Isot. 55 (2), 267–272. https://doi.org/10.1016/S0969-8043(00)00387-0.
Planinić, J., Vuković, B., Radolić, V., 2004. Radon time variations and deterministic chaos. J. Environ. Radioact. 75 (1), 35–45. https://doi.org/10.1016/j.jenvrad.2003.10.007.
Pulinets, S., Boyarchuk, K., 2004. Ionospheric Precursors of Earthquakes. Springer Science & Business Media.
Pulinets, S., Ouzounov, D., 2011. Lithosphere–Atmosphere–Ionosphere Coupling (LAIC) model–An unified concept for earthquake precursors validation. J. Asian Earth Sci. 41 (4–5), 371–382. https://doi.org/10.1016/j.jseaes.2010.03.005.
Ramola, R.C., Prasad, Y., Prasad, G., Kumar, S., Choubey, V.M., 2008. Soil-gas radon as seismotectonic indicator in Garhwal Himalaya. Appl. Radiat. Isot. 66 (10), 1523–1530. https://doi.org/10.1016/j.apradiso.2008.04.006.
Rehman, K., Ali, A., Ahmed, S., Ali, W., Ali, A., Khan, M.Y., 2015. Spatio-temporal variations of b-value in and around north Pakistan. Journal of Earth System Science 124 (7), 1445–1456. https://doi.org/10.1007/s12040-015-0625-2.
Rehman, K., Ali, W., Ali, A., Ali, A., Barkat, A., 2017a. Shallow and intermediate depth earthquakes in the Hindu Kush region across the Afghan-Pakistan border. J. Asian Earth Sci. 148, 241–253. https://doi.org/10.1016/j.jseaes.2017.09.005.
Rehman, K., Burton, P.W., Weatherill, G.A., 2017b. Application of Gumbel I and Monte Carlo methods to assess seismic hazard in and around Pakistan. J. Seismol. https://doi.org/10.1007/s10950-017-9723-8.
Riggio, A., Santulin, M., 2015. Earthquake Forecasting: a review of radon as seismic precursor. Boll. Geofis. Teor. Appl. 56 (2), 95–114. https://doi.org/10.4430/bgta0148.
Sharma, N., Singh, J., Esakki, S.C., Tripathi, R.M., 2016. A study of the natural radioactivity and radon exhalation rate in some cements used in India and its radiological significance. Journal of Radiation Research and Applied Sciences 9 (1), 47–56. https://doi.org/10.1016/j.jrras.2015.09.001.
Siddique, N.A.I.L.A., Rahman, A.S.M.A., 2006. Measurement of radionuclides in contaminated environmental matrices: Participation in Quality Assessment Programme (QAP) of US Department of Energy's Environmental Monitoring Laboratory. J. Radioanal. Nucl. Chem. 268 (3), 579–598. https://doi.org/10.1556/JRNC.268.2006.3.21.
Singh, S., Rani, A., Mahajan, R.K., 2005a. ^{226}Ra, ^{232}Th and ^{40}K analysis in soil samples from some areas of Punjab and Himachal Pradesh, India using gamma ray spectrometry. Radiat. Meas. 39 (4), 431–439. https://doi.org/10.1016/j.radmeas.2004.09.003.
Singh, K., Singh, M., Singh, S., Sahota, H.S., Papp, Z., 2005b. Variation of radon (^{222}Rn) progeny concentrations in outdoor air as a function of time, temperature and relative humidity. Radiat. Meas. 39 (2), 213–217. https://doi.org/10.1016/j.radmeas.2004.06.015.
Singh, S., Jaishi, H.P., Tiwari, R.P., Tiwari, R.C., 2017. Time series analysis of soil radon data using multiple linear regression and artificial neural network in seismic precursory studies. Pure Appl. Geophys. 1–10. https://doi.org/10.1007/s00024-017-1556-4.
Sroor, A., El-Bahi, S.M., Ahmed, F., Abdel-Haleem, A.S., 2001. Natural radioactivity and radon exhalation rate of soil in southern Egypt. Appl. Radiat. Isot. 55 (6), 873–879. https://doi.org/10.1016/S0969-8043(01)00123-3.

Sugisaki, R., 1978. Changing He/Ar and N_2/Ar ratios of fault air may be earthquake precursors. Nature 275 (5677), 209.
Tahir, M., Grasso, J.R., 2013. Aftershock patterns of ms > 7 earthquakes in the India–Asia collision belt: anomalous results from the Muzaffarabad earthquake sequence, Kashmir, 2005. Bull. Seismol. Soc. Am. 104 (1), 1–23. https://doi.org/10.1785/0120120158.
Tarakçı, M., Harmanşah, C., Saç, M.M., İçhedef, M., 2014. Investigation of the relationships between seismic activities and radon level in Western Turkey. Appl. Radiat. Isot. 83, 12–17. https://doi.org/10.1016/j.apradiso.2013.10.008.
Tatli, H., 2015. Detecting persistence of meteorological drought via the Hurst exponent. Meteorol. Appl. 22 (4), 763–769. https://doi.org/10.1002/met.1519.
Vaupotic, J., Riggio, A., Santulin, M., Zmazek, B., Kobal, I., 2010. A radon anomaly in soil gas at Cazzaso, NE Italy, as a precursor of an ML= 5.1earthquake. Nukleonika 55, 507–511.
Vinson, D.S., Vengosh, A., Hirschfeld, D., Dwyer, G.S., 2009. Relationships between radium and radon occurrence and hydrochemistry in fresh groundwater from fractured crystalline rocks, North Carolina (USA). Chem. Geol. 260 (3–4), 159–171. https://doi.org/10.1016/j.chemgeo.2008.10.022.
Walia, V., Yang, T.F., Lin, S.J., Kumar, A., Fu, C.C., Chiu, J.M., Chen, C.H., 2013. Temporal variation of soil gas compositions for earthquake surveillance in Taiwan. Radiat. Meas. 50, 154–159. https://doi.org/10.1016/j.radmeas.2012.11.007.
Wang, Y., Hilton, D.R., Zhou, Z., Zheng, G., 2017. Progress in the application of gas geochemistry to geothermal. Tectonic and Magmatic Studies. https://doi.org/10.1016/j.chemgeo.2017.08.026.
Woith, H., 2015. Radon earthquake precursor: a short review. Eur. Phys. J. Spec. Top. 224 (4), 611–627. http://doi.org/10.1140/epjst/e2015-02395-9.
Yan, R., Woith, H., Wang, R., Wang, G., 2018. 40-year record of radon, water temperature, and discharge rate from a hot spring in China. GFZ Data Services: Potsdam. http://doi.org/10.5880/GFZ.2.1.2018.002.
Yang, T.F., Walia, V., Chyi, L.L., Fu, C.C., Chen, C.H., Liu, T.K., Lee, M., 2005. Variations of soil radon and thoron concentrations in a fault zone and prospective earthquakes in SW Taiwan. Radiat. Meas. 40 (2), 496–502. https://doi.org/10.1016/j.radmeas.2005.05.017.
Yuce, G., Fu, C.C., D'Alessandro, W., Gulbay, A.H., Lai, C.W., Bellomo, S., Walia, V., 2017. Geochemical characteristics of soil radon and carbon dioxide within the dead sea Fault and karasu fault in the amik basin (Hatay), Turkey. Chem. Geol. 469, 129–146. https://doi.org/10.1016/j.chemgeo.2017.01.003.
Zafrir, H., Ben Horin, Y., Malik, U., Chemo, C., Zalevsky, Z., 2016. Novel determination of radon-222 velocity in deep subsurface rocks and the feasibility to using radon as an earthquake precursor. J. Geophys. Res.: Solid Earth 121 (9), 6346–6364. https://doi.org/10.1002/2016JB013033.
Zmazek, B., Živčić, M., Todorovski, L., Džeroski, S., Vaupotič, J., Kobal, I., 2005. Radon in soil gas: how to identify anomalies caused by earthquakes. Appl. Geochem. 20 (6), 1106–1119. https://doi.org/10.1016/j.apgeochem.2005.01.014.